

# Geometry-Aware Variational Autoencoders for Medical Data Augmentation.

Stéphanie Allasonnière\*  
join work with Clément Chadebec\*  
& Ninon Burgos† & Elina Thibeau-Sutre†

\*Université de Paris - INRIA HeKA - INSERM

†INRIA Aramis - Institut du Cerveau - CNRS



# Overview

- 1 Introduction
- 2 Variational Auto-Encoder - The Idea
  - Auto-Encoder
- 3 VAE framework
  - The idea
  - Mathematical foundations
  - Tweaking the approximate posterior distribution
- 4 Toward a Geometry-Aware VAE
  - The framework
  - The proposed model
  - A new way to generate data
  - Sensitivities and robustness on toy data
- 5 Results on Neuroimaging data
  - Materials
  - Methods
  - Results

# Main Challenges

Main challenges with medical data

- Small number of subjects:
  - potential poor population representativity
  - no statistically significant results
  - overfitting

# Main Challenges

Main challenges with medical data

- Small number of subjects:
  - potential poor population representativity
  - no statistically significant results
  - overfitting
- Large data (e.g. MRIs, omic data, etc..)  $\implies$  thousands of dimensions

# Main Challenges

## Main challenges with medical data

- Small number of subjects:
  - potential poor population representativity
  - no statistically significant results
  - overfitting
- Large data (e.g. MRIs, omic data, etc..)  $\implies$  thousands of dimensions

## Need for

- Dimensionality reduction

# Main Challenges

## Main challenges with medical data

- Small number of subjects:
  - potential poor population representativity
  - no statistically significant results
  - overfitting
- Large data (e.g. MRIs, omic data, etc..)  $\implies$  thousands of dimensions

## Need for

- Dimensionality reduction  
OR
- Data augmentation

# Main Challenges

## Main challenges with medical data

- Small number of subjects:
  - potential poor population representativity
  - no statistically significant results
  - overfitting
- Large data (e.g. MRIs, omic data, etc..)  $\implies$  thousands of dimensions

## Need for

- Dimensionality reduction  
OR /AND
- Data augmentation

# Main Challenges

## Main challenges with medical data

- Small number of subjects:
  - potential poor population representativity
  - no statistically significant results
  - overfitting
- Large data (e.g. MRIs, omic data, etc..)  $\implies$  thousands of dimensions

## Need for

- Dimensionality reduction  
OR
- Data augmentation

## A solution?

- Generative models: statistical hierarchical OR neural network based models

# Main Challenges

## Main challenges with medical data

- Small number of subjects:
  - potential poor population representativity
  - no statistically significant results
  - overfitting
- Large data (e.g. MRIs, omic data, etc..)  $\implies$  thousands of dimensions

## Need for

- Dimensionality reduction  
OR
- Data augmentation

## A solution?

- Generative models: statistical hierarchical OR neural network based models

## Issue

- Most of the time, unable to generate faithfully **with small data sets**

# Classic Data Augmentation

- Adding some geometric transformations (shift, rotations ...)
- Adding noise, blur ...

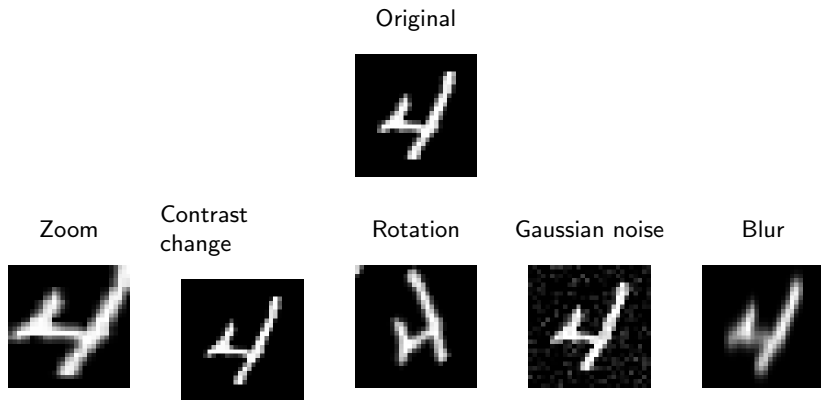


Figure: Examples of transformations

# Classic Data Augmentation - Shortcomings

## Classic DA

- Is data set dependent
- May require the intervention of an expert “knowledge”



Figure: Nine figure rotated.

# Classic Data Augmentation - Shortcomings

## Classic DA

- Is data set dependent
- May require the intervention of an expert “knowledge”



Figure: Nine figure rotated.

## An attractive solution?

- **Generative models** (Generative Adversarial Networks, Variational Auto-Encoders ...)

# Use of Generative Models for DA

**GANs:** wide use in many fields of application including medicine [YWB19]:

- Magnetic Resonance Images (MRI) [STR<sup>+</sup>18, CMST17]
- Computed Tomography (CT) [FADK<sup>+</sup>18, SYPS19]
- X-ray [MMKSM18, SVD<sup>+</sup>18, WGG<sup>+</sup>20],
- Positron Emission Tomography (PET) [BKK<sup>+</sup>17],
- Mass spectroscopy data [LZL<sup>+</sup>19],
- Dermoscopy [BAN18]
- Mammography [KRO<sup>+</sup>18, WWCL18]

# Use of Generative Models for DA

**GANs:** wide use in many fields of application including medicine [YWB19]:

- Magnetic Resonance Images (MRI) [STR<sup>+</sup>18, CMST17]
- Computed Tomography (CT) [FADK<sup>+</sup>18, SYPS19]
- X-ray [MMKSM18, SVD<sup>+</sup>18, WGG<sup>+</sup>20],
- Positron Emission Tomography (PET) [BKK<sup>+</sup>17],
- Mass spectroscopy data [LZL<sup>+</sup>19],
- Dermoscopy [BAN18]
- Mammography [KRO<sup>+</sup>18, WWCL18]

⇒ Most of these studies involved either a quite **large training set** (above 1000 training samples) or quite **small dimensional data**.

⇒ As of today, the HDLSS setting remains poorly explored.

# Use of Generative Models for DA

**GANs:** wide use in many fields of application including medicine [YWB19]:

- Magnetic Resonance Images (MRI) [STR<sup>+</sup>18, CMST17]
- Computed Tomography (CT) [FADK<sup>+</sup>18, SYPS19]
- X-ray [MMKSM18, SVD<sup>+</sup>18, WGG<sup>+</sup>20],
- Positron Emission Tomography (PET) [BKK<sup>+</sup>17],
- Mass spectroscopy data [LZL<sup>+</sup>19],
- Dermoscopy [BAN18]
- Mammography [KRO<sup>+</sup>18, WWCL18]

⇒ Most of these studies involved either a quite **large training set** (above 1000 training samples) or quite **small dimensional data**.

⇒ As of today, the HDLSS setting remains poorly explored.

⇒ **Use VAEs!**

# Auto-Encoder

- The objective  $\implies$  Dimensionality Reduction

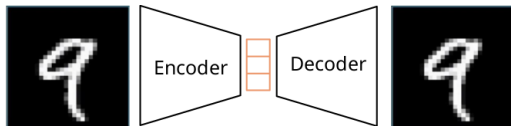


Figure: Simple Auto-Encoder

- Need for a representation of the image  $\implies$  vectors

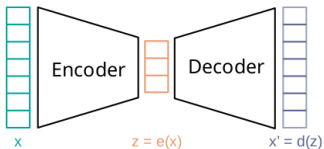


Figure: Simple Auto-Encoder

# AutoEncoder

Assumptions:

- Let  $x \in \mathcal{X}$  be a set a data. We assume that there exists  $z \in \mathcal{Z}$  such that  $z$  is a low dimensional representation of  $x$
- The encoder  $e_\theta$  and decoder  $d_\phi$  are functions modelled by neural networks (NNs) such that  $\theta$  and  $\phi$  are the weights of the NNs
- Let  $x'$  be the reconstructed samples, the objective is to have  $x \simeq x'$

The Objective function writes:

$$\mathcal{L} = \|x - x'\|^2 = \|x - d_\phi(z)\|^2 = \|x - d_\phi(e_\theta(x))\|^2$$

# AutoEncoder

Assumptions:

- Let  $x \in \mathcal{X}$  be a set a data. We assume that there exists  $z \in \mathcal{Z}$  such that  $z$  is a low dimensional representation of  $x$
- The encoder  $e_\theta$  and decoder  $d_\phi$  are functions modelled by neural networks (NNs) such that  $\theta$  and  $\phi$  are the weights of the NNs
- Let  $x'$  be the reconstructed samples, the objective is to have  $x \simeq x'$

The Objective function writes:

$$\mathcal{L} = \|x - x'\|^2 = \|x - d_\phi(z)\|^2 = \|x - d_\phi(e_\theta(x))\|^2$$

$\implies$  The networks are optimised using stochastic gradient descent

$$\phi \leftarrow \phi - \varepsilon \cdot \nabla_\phi \mathcal{L}$$

$$\theta \leftarrow \theta - \varepsilon \cdot \nabla_\theta \mathcal{L}$$

# AutoEncoder - Shortcomings

- How to generate new data ?

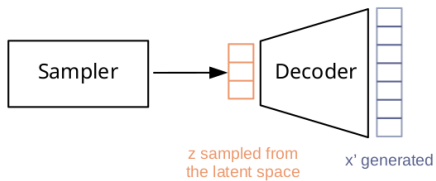


Figure: Generation procedure ?

# AutoEncoder - Shortcomings

- How to generate new data ?

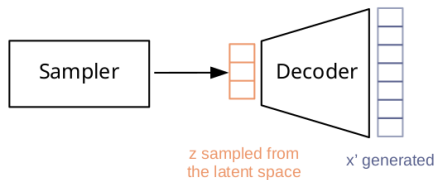


Figure: Generation procedure ?

- How to sample form the latent space?

# AutoEncoder - Shortcomings

- How to generate new data ?

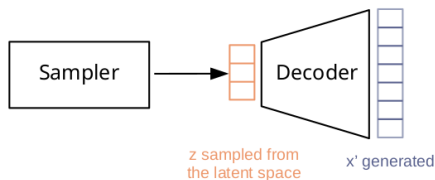


Figure: Generation procedure ?

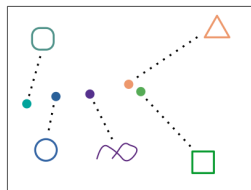


Figure: Potential latent space

- How to sample form the latent space?
- The AutoEncoder was just trained to **encode and decode the input data** without information on its structure or distribution.

# AutoEncoder - Shortcomings

- How to generate new data ?

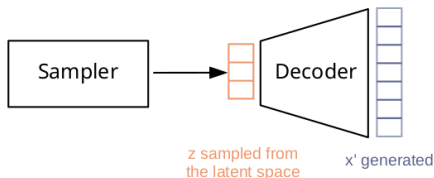


Figure: Generation procedure ?

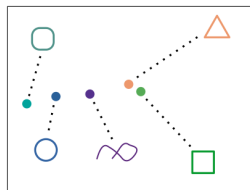


Figure: Potential latent space

- How to sample form the latent space?
- The AutoEncoder was just trained to **encode and decode the input data** without information on its structure or distribution.

⇒ Need for a new framework

# VAE - The Idea

- An auto-encoder based model...

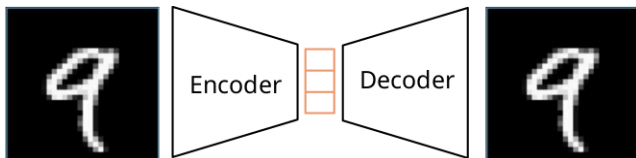


Figure: Simple Auto-Encoder

- ... but where an input data point is encoded as a **distribution** defined over the latent space [KW14, RMW14]

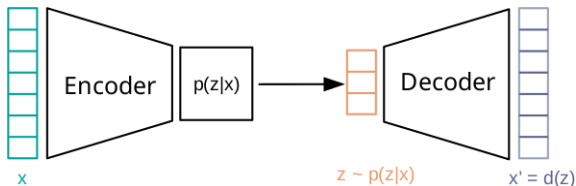


Figure: VAE framework

# VAE - Mathematical Considerations

- Let  $x \in \mathcal{X}$  be a set of data and  $\{P_\theta, \theta \in \Theta\}$  be a parametric model

# VAE - Mathematical Considerations

- Let  $x \in \mathcal{X}$  be a set of data and  $\{P_\theta, \theta \in \Theta\}$  be a parametric model
- We assume there exists latent variables  $z \in \mathcal{Z}$  living in a smaller space such that the marginal likelihood writes

$$p_\theta(x) = \int p_\theta(x|z)q_{\text{prior}}(z)dz,$$

where  $q_{\text{prior}}$  is a prior distribution over the latent variables and  $p_\theta(x|z)$  is referred to as the decoder

# VAE - Mathematical Considerations

- Let  $x \in \mathcal{X}$  be a set of data and  $\{P_\theta, \theta \in \Theta\}$  be a parametric model
- We assume there exists latent variables  $z \in \mathcal{Z}$  living in a smaller space such that the marginal likelihood writes

$$p_\theta(x) = \int p_\theta(x|z)q_{\text{prior}}(z)dz,$$

where  $q_{\text{prior}}$  is a prior distribution over the latent variables and  $p_\theta(x|z)$  is referred to as the decoder

- Example:

$$q_{\text{prior}} = \mathcal{N}(0, I), \quad p_\theta(x|z) = \prod_{i=1}^D \mathcal{B}(\pi_{\theta_i}(z))$$

# VAE - Mathematical Considerations

- Let  $x \in \mathcal{X}$  be a set of data and  $\{P_\theta, \theta \in \Theta\}$  be a parametric model
- We assume there exists latent variables  $z \in \mathcal{Z}$  living in a smaller space such that the marginal likelihood writes

$$p_\theta(x) = \int p_\theta(x|z)q_{\text{prior}}(z)dz,$$

where  $q_{\text{prior}}$  is a prior distribution over the latent variables and  $p_\theta(x|z)$  is referred to as the decoder

- Example:

$$q_{\text{prior}} = \mathcal{N}(0, I), \quad p_\theta(x|z) = \prod_{i=1}^D \mathcal{B}(\pi_{\theta_i}(z))$$

## Objective:

- Maximizing the likelihood of the model

# VAE - Mathematical Considerations

- Let  $x \in \mathcal{X}$  be a set of data and  $\{P_\theta, \theta \in \Theta\}$  be a parametric model
- We assume there exists latent variables  $z \in \mathcal{Z}$  living in a smaller space such that the marginal likelihood writes

$$p_\theta(x) = \int p_\theta(x|z)q_{\text{prior}}(z)dz,$$

where  $q_{\text{prior}}$  is a prior distribution over the latent variables and  $p_\theta(x|z)$  is referred to as the decoder

- Example:

$$q_{\text{prior}} = \mathcal{N}(0, I), \quad p_\theta(x|z) = \prod_{i=1}^D \mathcal{B}(\pi_{\theta_i}(z))$$

Objective:

- Maximizing the likelihood of the model

Problem: The integral is often intractable.

# Variational inference

We have to use Variational Inference:

$$\log p_{\theta}(x) = \log \left( \int p_{\theta}(x|z) q_{\text{prior}}(z) dz \right)$$

# Variational inference

We have to use Variational Inference:

$$\begin{aligned}\log p_{\theta}(x) &= \log \left( \int p_{\theta}(x|z) q_{\text{prior}}(z) dz \right) \\ &= \log \left( \int p_{\theta}(x, z) dz \right)\end{aligned}$$

# Variational inference

We have to use Variational Inference:

$$\begin{aligned}\log p_{\theta}(x) &= \log \left( \int p_{\theta}(x|z) q_{\text{prior}}(z) dz \right) \\ &= \log \left( \int p_{\theta}(x, z) dz \right) \\ &= \log \left( \int p_{\theta}(x, z) \frac{q(z)}{q(z)} dz \right), \text{ for any pdf } q\end{aligned}$$

# Variational inference

We have to use Variational Inference:

$$\begin{aligned}\log p_{\theta}(x) &= \log \left( \int p_{\theta}(x|z) q_{\text{prior}}(z) dz \right) \\ &= \log \left( \int p_{\theta}(x, z) dz \right) \\ &= \log \left( \int p_{\theta}(x, z) \frac{q(z)}{q(z)} dz \right), \text{ for any pdf } q \\ &\geq \int \left( \log \frac{p_{\theta}(x, z)}{q(z)} \right) q(z) dz, \text{ using Jensen's inequality}\end{aligned}$$

# Variational inference

We have to use Variational Inference:

$$\begin{aligned}\log p_{\theta}(x) &= \log \left( \int p_{\theta}(x|z) q_{\text{prior}}(z) dz \right) \\ &= \log \left( \int p_{\theta}(x, z) dz \right) \\ &= \log \left( \int p_{\theta}(x, z) \frac{q(z)}{q(z)} dz \right), \text{ for any pdf } q \\ &\geq \int \left( \log \frac{p_{\theta}(x, z)}{q(z)} \right) q(z) dz, \text{ using Jensen's inequality} \\ &\geq \int (\log p_{\theta}(x, z)) q(z) dz - H(q(z))\end{aligned}$$

with  $H$  the entropy of  $q(z)$ .

# Variational inference

We have to use Variational Inference:

$$\begin{aligned}\log p_{\theta}(x) &= \log \left( \int p_{\theta}(x|z) q_{\text{prior}}(z) dz \right) \\ &= \log \left( \int p_{\theta}(x, z) dz \right) \\ &= \log \left( \int p_{\theta}(x, z) \frac{q(z)}{q(z)} dz \right), \text{ for any pdf } q \\ &\geq \int \left( \log \frac{p_{\theta}(x, z)}{q(z)} \right) q(z) dz, \text{ using Jensen's inequality} \\ &\geq \int (\log p_{\theta}(x, z)) q(z) dz - H(q(z))\end{aligned}$$

with  $H$  the entropy of  $q(z)$ .

The equality holds for  $q(z) = q_{\theta}(z|x)$ .

## Variational inference: The ELBO

- Well-know issue: the posterior  $q(z) = q_{\theta}(z|x)$  is intractable.  
→ use Expectation-Maximization algorithms (up to the MCMC-SAEM version)
- **OR** approximate this posterior → ELBO

# Variational inference: The ELBO

- Well-know issue: the posterior  $q(z) = q_\theta(z|x)$  is intractable.  
→ use Expectation-Maximization algorithms (up to the MCMC-SAEM version)
- **OR** approximate this posterior → ELBO
- Introduce a parametric approximation:

$$q_\phi(z|x) \simeq p_\theta(z|x),$$

where  $q_\phi(z|x) = \mathcal{N}(\mu_\phi(x), \Sigma_\phi(x))$

# Variational inference: The ELBO

- Well-known issue: the posterior  $q(z) = q_\theta(z|x)$  is intractable.  
→ use Expectation-Maximization algorithms (up to the MCMC-SAEM version)
- **OR** approximate this posterior → ELBO
- Introduce a parametric approximation:

$$q_\phi(z|x) \simeq p_\theta(z|x),$$

where  $q_\phi(z|x) = \mathcal{N}(\mu_\phi(x), \Sigma_\phi(x))$

- This leads to an unbiased estimate of the log-likelihood

$$\hat{p}_\theta(x) = \frac{p_\theta(x, z)}{q_\phi(z|x)}, \quad \mathbb{E}_{z \sim q_\phi(z|x)}[\hat{p}_\theta(x)] = p_\theta(x),$$

# Variational inference: The ELBO

- Well-know issue: the posterior  $q(z) = q_\theta(z|x)$  is intractable.  
 → use Expectation-Maximization algorithms (up to the MCMC-SAEM version)
- OR** approximate this posterior → ELBO
- Introduce a parametric approximation:

$$q_\phi(z|x) \simeq p_\theta(z|x),$$

where  $q_\phi(z|x) = \mathcal{N}(\mu_\phi(x), \Sigma_\phi(x))$

- This leads to an unbiased estimate of the log-likelihood

$$\hat{p}_\theta(x) = \frac{p_\theta(x, z)}{q_\phi(z|x)}, \quad \mathbb{E}_{z \sim q_\phi(z|x)}[\hat{p}_\theta(x)] = p_\theta(x),$$

- and the definition of the **Evidence Lower Bound** (ELBO):

$$\begin{aligned} \log p_\theta(x) &\geq \mathbb{E}_{z \sim q_\phi(z|x)}[\log(p_\theta(x, z)) - \log(q_\phi(z|x))] \\ &\geq \text{ELBO} \end{aligned}$$

# Variational inference: The ELBO

## Objectives:

1. Optimize the ELBO **as a function** instead of the target distribution  
Use stochastic gradient descent in both  $\theta$  and  $\phi$

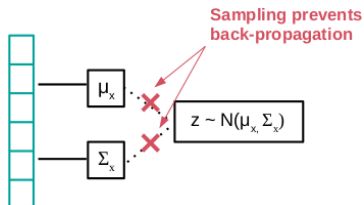
# Variational inference: The ELBO

## Objectives:

1. Optimize the ELBO **as a function** instead of the target distribution  
Use stochastic gradient descent in both  $\theta$  and  $\phi$
2. Optimize the ELBO **as a bound** to get closer to the target  
Use sampling methods to produce samples  $z \sim q_{\theta}(z|x)$

# The Reparametrization Trick for stochastic gradient descent

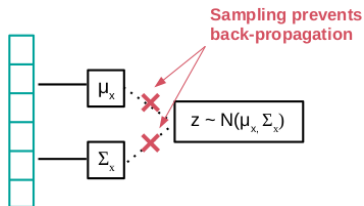
- Since  $z \sim \mathcal{N}(\mu_\phi(x), \Sigma_\phi(x))$ , the model is not amenable to gradient descent



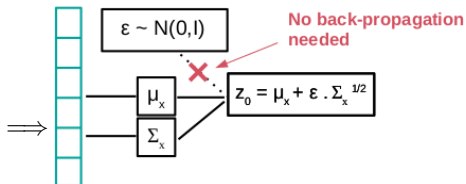
(a) Back-propagation impossible

# The Reparametrization Trick for stochastic gradient descent

- Since  $z \sim \mathcal{N}(\mu_\phi(x), \Sigma_\phi(x))$ , the model is not amenable to gradient descent



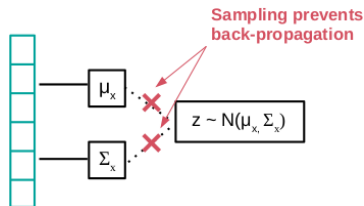
(a) Back-propagation impossible



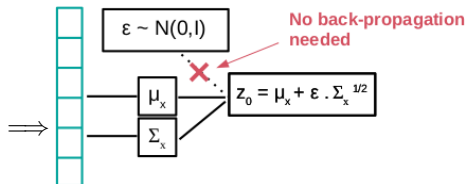
(b) Back-propagation possible

# The Reparametrization Trick for stochastic gradient descent

- Since  $z \sim \mathcal{N}(\mu_\phi(x), \Sigma_\phi(x))$ , the model is not amenable to gradient descent



(a) Back-propagation impossible



(b) Back-propagation possible

$\Rightarrow$  Optimization with respect to encoder and decoder parameters made possible !

## Objective 1.



# Generating new samples

- We only need to sample  $z \sim \mathcal{N}(0, I)$  and feed it to the decoder.

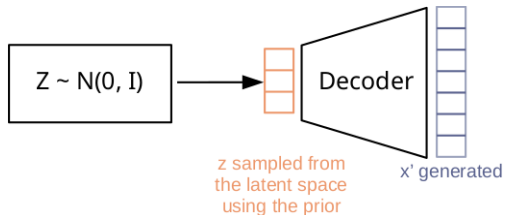


Figure: Generation procedure using prior

## Generating new samples

- We only need to sample  $z \sim \mathcal{N}(0, I)$  and feed it to the decoder.

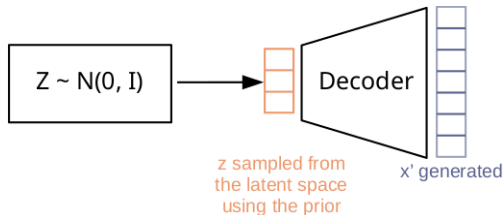


Figure: Generation procedure using prior

### Pros:

- Very simple to use in practice

# Generating new samples

- We only need to sample  $z \sim \mathcal{N}(0, I)$  and feed it to the decoder.

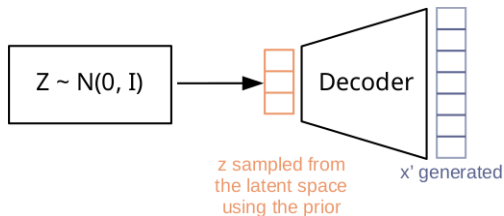


Figure: Generation procedure using prior

## Pros:

- Very simple to use in practice

## Cons:

- The prior and posterior are **not expressive enough** to capture complex distributions
- **Poor latent space prospecting**

# Tweaking the Approximate Posterior Distribution

## Concerning Objective 2.

- The ELBO can be written as

$$ELBO = \log p_{\theta}(x) - \underbrace{\text{KL}(q_{\phi}(z|x) || p_{\theta}(z|x))}_{\approx 0 \text{ if } q_{\phi}(z|x) \approx p_{\theta}(z|x)}.$$

- Kullback-Leiber divergence  $\geq 0 \Rightarrow$  make it vanish by tweaking the approximate posterior  $q_{\phi}(z|x)$
- Produce variables  $z$  which targets the true posterior  $p_{\theta}(z|x)$  using a sample  $z_0 \sim q_{init}$

# Tweaking the Approximate Posterior Distribution

## Concerning Objective 2.

- The ELBO can be written as

$$ELBO = \log p_{\theta}(x) - \underbrace{\text{KL}(q_{\phi}(z|x) || p_{\theta}(z|x))}_{\approx 0 \text{ if } q_{\phi}(z|x) \approx p_{\theta}(z|x)}.$$

- Kullback-Leiber divergence  $\geq 0 \Rightarrow$  make it vanish by tweaking the approximate posterior  $q_{\phi}(z|x)$
- Produce variables  $z$  which targets the true posterior  $p_{\theta}(z|x)$  using a sample  $z_0 \sim q_{init}$
- How? and how to ensure that the model would still be amenable to the back-propagation ?

## Solution 1: Normalizing Flows

- Use smooth invertible parametrized mappings  $f_\psi$  to “sample”  $z$  [RM15]
- Apply  $K$  transformations to  $z_0 \sim q_{init}$  (here  $q_{init} = q_\phi$ )
- Final random variable  $z_K = f_x^K \circ \dots \circ f_x^1(z_0) \sim q_\phi(z_K|x)$  with

$$q_\phi(z_K|x) = q_\phi(z_0|x) \prod_{k=1}^K |\det \mathbf{J}_{f_x^k}|^{-1}, \quad (1)$$

## Solution 1: Normalizing Flows

- Use smooth invertible parametrized mappings  $f_\psi$  to “sample”  $z$  [RM15]
- Apply  $K$  transformations to  $z_0 \sim q_{init}$  (here  $q_{init} = q_\phi$ )
- Final random variable  $z_K = f_x^K \circ \dots \circ f_x^1(z_0) \sim q_\phi(z_K|x)$  with

$$q_\phi(z_K|x) = q_\phi(z_0|x) \prod_{k=1}^K |\det \mathbf{J}_{f_x^k}|^{-1}, \quad (1)$$

### Objective 2.



although difficult to compute the Jacobian of these maps  $f_1^K$

## Solution 2: Hamiltonian VAE

- Idea = Hybrid Monte Carlo Sampler [No11, DMS17, LBB<sup>+</sup>19],
- Target density

$$p_{\theta}(z|x) = \frac{p_{\theta}(x, z)}{p_{\theta}(x)} \propto p_{\theta}(x, z) = \pi_x(z).$$

- Introduce an auxiliary random variable  $\rho \sim \mathcal{N}(0, \mathbf{M})$  called “momentum”
- Write the Hamiltonian:

$$\begin{aligned} H_x(z, \rho) &= -\log \pi_x(z, \rho) \\ &= -\log \pi_x(z) + \frac{1}{2} \log((2\pi)^d |\mathbf{M}|) + \rho^{\top} \mathbf{M}^{-1} \rho \\ &= U_x(z) + \kappa(\rho). \end{aligned}$$

- Sample  $(z, \rho)$  with this dynamic.

## Solution 2: Hamiltonian VAE

- Use a discretization scheme

$$\begin{aligned}\rho(t + \varepsilon/2) &= \rho(t) - \frac{\varepsilon}{2} \cdot \nabla_z H(z(t), \rho(t)), \\ z(t + \varepsilon) &= z(t) + \varepsilon \cdot \nabla_\rho (H(z(t), \rho(t + \varepsilon/2))), \\ \rho(t + \varepsilon) &= \rho(t + \varepsilon/2) - \frac{\varepsilon}{2} \cdot \nabla_z H(z(t + \varepsilon), \rho(t + \varepsilon/2)),\end{aligned}\tag{2}$$

- A proposal  $(\tilde{z}, \tilde{\rho})$  is accepted with probability:

$$\alpha = \min\left(1, \exp\left(-H(\tilde{z}, \tilde{\rho}) + H(z, \rho)\right)\right)$$

⇒ Creates an ergodic, time-reversible Markov Chain having  $\pi_x$  as stationary distribution.

# Hamiltonian VAE

- The graphical scheme [CDS18]

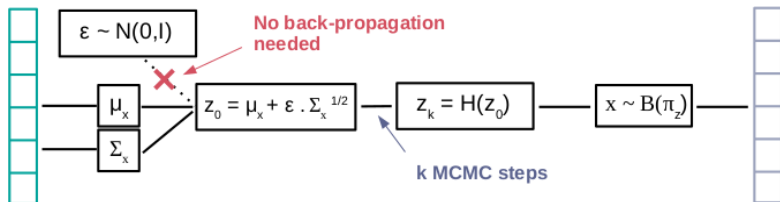


Figure: Hamiltonian VAE

# Hamiltonian VAE

- The graphical scheme [CDS18]

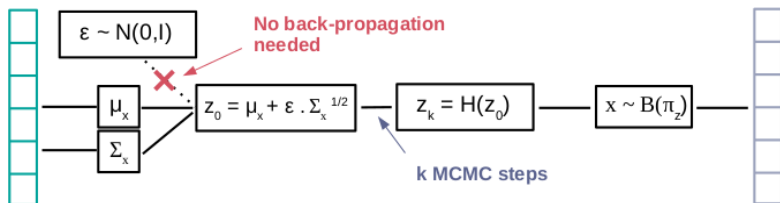


Figure: Hamiltonian VAE

# Hamiltonian VAE

- The graphical scheme [CDS18]

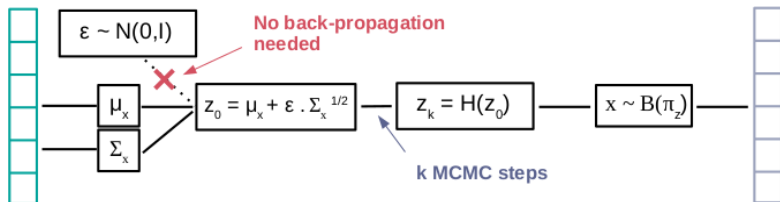


Figure: Hamiltonian VAE

Issue: Perform poorly when trained on small data set and so we need to define a new framework

What about geometry?

# Defining a New Framework

Assumptions:

- As of now the latent space structure was supposed to be Euclidean (i.e.  $\mathcal{Z} = \mathbb{R}^d$ )

# Defining a New Framework

Assumptions:

- As of now the latent space structure was supposed to be Euclidean (i.e.  $\mathcal{Z} = \mathbb{R}^d$ )
- Let us now relax this hypothesis and assume that  $\mathcal{Z}$  is a Riemannian manifold endowed with a metric  $\mathbf{G}$ .

# Defining a New Framework

Assumptions:

- As of now the latent space structure was supposed to be Euclidean (i.e.  $\mathcal{Z} = \mathbb{R}^d$ )
- Let us now relax this hypothesis and assume that  $\mathcal{Z}$  is a Riemannian manifold endowed with a metric  $\mathbf{G}$ .
- It was shown that exploiting the geometrical aspect of probability distributions can lead to far more efficient sampling [GCC09, GC11]

# Defining a New Framework

## Assumptions:

- As of now the latent space structure was supposed to be Euclidean (i.e.  $\mathcal{Z} = \mathbb{R}^d$ )
- Let us now relax this hypothesis and assume that  $\mathcal{Z}$  is a Riemannian manifold endowed with a metric  $\mathbf{G}$ .
- It was shown that exploiting the geometrical aspect of probability distributions can lead to far more efficient sampling [GCC09, GC11]

## Our ideas:

- 1 Exploit the manifold structure of the latent space to improve the posterior sampling [CMA20]

# Defining a New Framework

## Assumptions:

- As of now the latent space structure was supposed to be Euclidean (i.e.  $\mathcal{Z} = \mathbb{R}^d$ )
- Let us now relax this hypothesis and assume that  $\mathcal{Z}$  is a Riemannian manifold endowed with a metric  $\mathbf{G}$ .
- It was shown that exploiting the geometrical aspect of probability distributions can lead to far more efficient sampling [GCC09, GC11]

## Our ideas:

- 1 Exploit the manifold structure of the latent space to improve the posterior sampling [CMA20]
- 2 Learn the metric defined in the latent space [CMA20]

# Defining a New Framework

## Assumptions:

- As of now the latent space structure was supposed to be Euclidean (i.e.  $\mathcal{Z} = \mathbb{R}^d$ )
- Let us now relax this hypothesis and assume that  $\mathcal{Z}$  is a Riemannian manifold endowed with a metric  $\mathbf{G}$ .
- It was shown that exploiting the geometrical aspect of probability distributions can lead to far more efficient sampling [GCC09, GC11]

## Our ideas:

- 1 Exploit the manifold structure of the latent space to improve the posterior sampling [CMA20]
- 2 Learn the metric defined in the latent space [CMA20]
- 3 Use the learned geometry to generate instead of the prior [CTSBA21]

# Riemanian geometry principles

- Riemanian manifold: (reduced to our model)  $\mathbb{R}^d$  endowed with a metric  $\mathbf{G}$ :  
 $\mathcal{M} = (\mathbb{R}^d, \mathbf{G})$ .  
 $\implies \mathbb{R}^d$  not flat anymore, curved space (as montains)

# Riemanian geometry principles

- Riemanian manifold: (reduced to our model)  $\mathbb{R}^d$  endowed with a metric  $\mathbf{G}$ :  
 $\mathcal{M} = (\mathbb{R}^d, \mathbf{G})$ .  
 $\implies \mathbb{R}^d$  not flat anymore, curved space (as montains)
- Geodesic curves:
  - Length of a curve  $\gamma : [0, 1] \rightarrow \mathcal{M}$  from  $z_1$  to  $z_2$  living in a Riemannian manifold  $\mathcal{M}$

$$L(\gamma) = \int_0^1 \sqrt{\langle \gamma'(t), \gamma'(t) \rangle_{\gamma(t)}} dt \quad \gamma(0) = z_1, \gamma(1) = z_2. \quad (3)$$

- Geodesic paths = curve  $\gamma$  minimizing Eq. (3)

# Riemanian geometry principles

- Riemanian manifold: (reduced to our model)  $\mathbb{R}^d$  endowed with a metric  $\mathbf{G}$ :  
 $\mathcal{M} = (\mathbb{R}^d, \mathbf{G})$ .  
 $\implies \mathbb{R}^d$  not flat anymore, curved space (as montains)
- Geodesic curves:
  - Length of a curve  $\gamma : [0, 1] \rightarrow \mathcal{M}$  from  $z_1$  to  $z_2$  living in a Riemannian manifold  $\mathcal{M}$

$$L(\gamma) = \int_0^1 \sqrt{\langle \gamma'(t), \gamma'(t) \rangle_{\gamma(t)}} dt \quad \gamma(0) = z_1, \gamma(1) = z_2. \quad (3)$$

- **Geodesic paths** = curve  $\gamma$  minimizing Eq. (3)
- or equivalently **minimizing the curve energy**

$$E(\gamma) = \int_0^1 \langle \gamma'(t), \gamma'(t) \rangle_{\gamma(t)} dt \quad \gamma(0) = z_1, \gamma(1) = z_2.$$

# Riemanian geometry principles

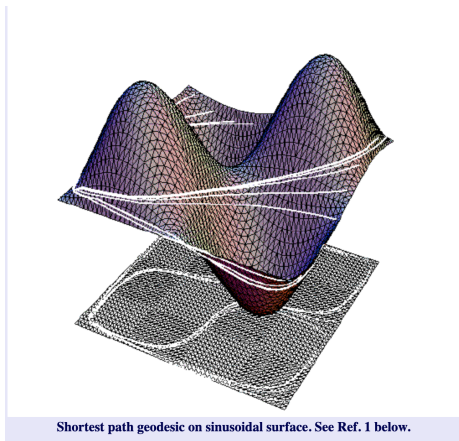


**Figure:** Image taken from: Fast Marching Methods on Triangulated Domains : Kimmel, R., and Sethian, J.A., Proceedings of the National Academy of Sciences, 95, pp. 8341-8435, 1998

# 1) Improve Posterior Sampling - Riemannian HMC

- The idea relies on the [Riemannian](#) Hamiltonian Monte Carlo Sampler [GC11]

# 1) Improve Posterior Sampling - Riemannian HMC

- The idea relies on the **Riemannian** Hamiltonian Monte Carlo Sampler [GC11]
- Simulates the evolution  $(z(t), v(t))$  of a particle whose motion is governed by Hamiltonian dynamics and having a potential  $U(z)$  and kinetic energy  $K(v, z)$

$$U(z) = -\log p_{\text{target}}(z), \quad K(v, z) = \frac{1}{2} v^\top \mathbf{G}^{-1}(z) v.$$

- **Position-specific** random momentum  $\rho \sim \mathcal{N}(0, \mathbf{G}(z))$  introduced
- The Hamiltonian writes

$$H_x^{\text{Riem}}(z, \rho) = U_x(z) + \frac{1}{2} \log((2\pi)^D \det \mathbf{G}(z)) + \frac{1}{2} \rho^\top \mathbf{G}(z)^{-1} \rho.$$

# 1) Improve Posterior Sampling - Riemannian HMC

- The idea relies on the **Riemannian** Hamiltonian Monte Carlo Sampler [GC11]
- Simulates the evolution  $(z(t), v(t))$  of a particle whose motion is governed by Hamiltonian dynamics and having a potential  $U(z)$  and kinetic energy  $K(v, z)$

$$U(z) = -\log p_{\text{target}}(z), \quad K(v, z) = \frac{1}{2} v^\top \mathbf{G}^{-1}(z) v.$$

- **Position-specific** random momentum  $\rho \sim \mathcal{N}(0, \mathbf{G}(z))$  introduced
- The Hamiltonian writes

$$H_x^{\text{Riem}}(z, \rho) = U_x(z) + \frac{1}{2} \log((2\pi)^D \det \mathbf{G}(z)) + \frac{1}{2} \rho^\top \mathbf{G}(z)^{-1} \rho.$$

- Use of the “Generalized” Leapfrog integrator to sample from  $p_{\text{target}}$

# 1) Improve Posterior Sampling - Riemannian HMC

- The idea relies on the **Riemannian** Hamiltonian Monte Carlo Sampler [GC11]
- Simulates the evolution  $(z(t), v(t))$  of a particle whose motion is governed by Hamiltonian dynamics and having a potential  $U(z)$  and kinetic energy  $K(v, z)$

$$U(z) = -\log p_{\text{target}}(z), \quad K(v, z) = \frac{1}{2} v^\top \mathbf{G}^{-1}(z) v.$$

- **Position-specific** random momentum  $\rho \sim \mathcal{N}(0, \mathbf{G}(z))$  introduced
- The Hamiltonian writes

$$H_x^{\text{Riem}}(z, \rho) = U_x(z) + \frac{1}{2} \log((2\pi)^D \det \mathbf{G}(z)) + \frac{1}{2} \rho^\top \mathbf{G}(z)^{-1} \rho.$$

- Use of the “Generalized” Leapfrog integrator to sample from  $p_{\text{target}}$

## Pros:

- Use the underlying geometry of the data to improve sampling

# 1) Improve Posterior Sampling - Riemannian HMC

- The idea relies on the **Riemannian** Hamiltonian Monte Carlo Sampler [GC11]
- Simulates the evolution  $(z(t), v(t))$  of a particle whose motion is governed by Hamiltonian dynamics and having a potential  $U(z)$  and kinetic energy  $K(v, z)$

$$U(z) = -\log p_{\text{target}}(z), \quad K(v, z) = \frac{1}{2} v^\top \mathbf{G}^{-1}(z) v.$$

- **Position-specific** random momentum  $\rho \sim \mathcal{N}(0, \mathbf{G}(z))$  introduced
- The Hamiltonian writes

$$H_x^{\text{Riem}}(z, \rho) = U_x(z) + \frac{1}{2} \log((2\pi)^D \det \mathbf{G}(z)) + \frac{1}{2} \rho^\top \mathbf{G}(z)^{-1} \rho.$$

- Use of the “Generalized” Leapfrog integrator to sample from  $p_{\text{target}}$

Pros:

- Use the underlying geometry of the data to improve sampling

Cons:

- **The metric is unknown**

## 2) Learn the Metric - The Choice of the Metric

- Parametric metric: [Lou19]:

$$\mathbf{G}^{-1}(z) = \sum_{i=1}^N L_{\psi_i} L_{\psi_i}^{\top} \exp\left(-\frac{\|z - c_i\|_2^2}{T^2}\right) + \lambda I_d,$$

- $L_{\psi_i}$  lower triangular matrices parametrized using neural networks
- $T$  temperature to smooth the metric
- $c_i$  centroids
- $\lambda$  regularization factor

## 2) Learn the Metric - The Choice of the Metric

- Parametric metric: [Lou19]:

$$\mathbf{G}^{-1}(z) = \sum_{i=1}^N L_{\psi_i} L_{\psi_i}^{\top} \exp\left(-\frac{\|z - c_i\|_2^2}{T^2}\right) + \lambda I_d,$$

- $L_{\psi_i}$  lower triangular matrices parametrized using neural networks
- $T$  temperature to smooth the metric
- $c_i$  centroids
- $\lambda$  regularization factor

### Pros:

- Closed-form expression of the inverse metric  $\implies$  useful for **geodesic computation**
- **Geodesics travel through most populated areas.**

# The Model - Riemannian Hamiltonian VAE

- The graphical scheme

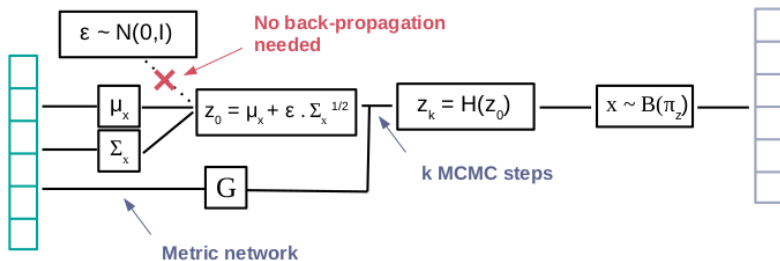
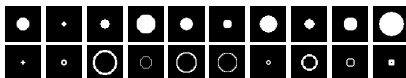


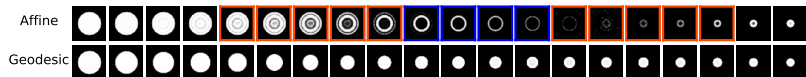
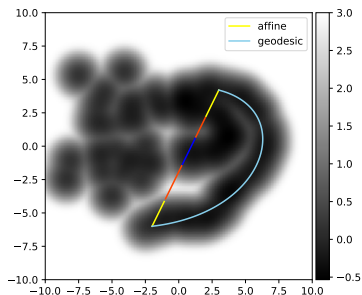
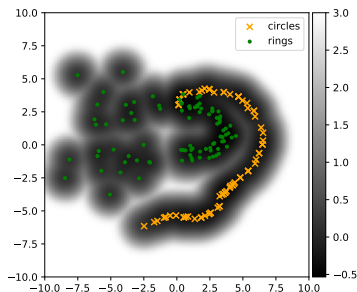
Figure: Riemannian Hamiltonian VAE.

# The Learned Latent Space examples

Training samples:



Latent space and interpolations:

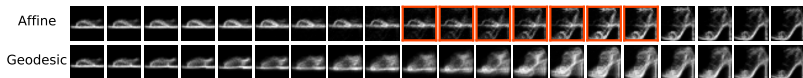
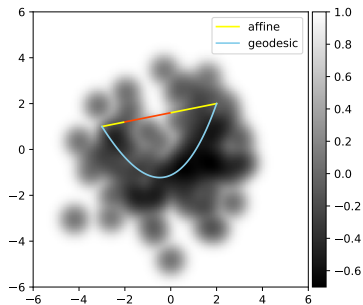
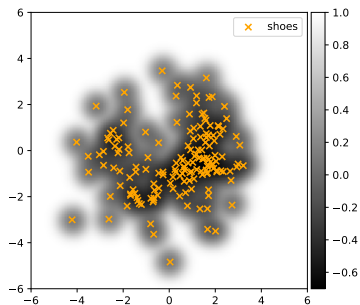


# The Learned Latent Space examples

Training samples:



Latent space and interpolations:



### 3) Improve Data Generation - Sample With the Metric

Idea:

- Use a geometry-based sampling procedure: pdf driven by the metric

$$p(z) = \frac{\mathbb{1}_S(z) \sqrt{\det \mathbf{G}^{-1}(z)}}{\int_{\mathbb{R}^d} \mathbb{1}_S(z) \sqrt{\det \mathbf{G}^{-1}(z)} dz},$$

where  $S$  is a compact set and  $\mathbb{1}_S(z) = 1$  if  $z \in S$ , 0 otherwise.

### 3) Improve Data Generation - Sample With the Metric

#### Idea:

- Use a geometry-based sampling procedure: pdf driven by the metric

$$p(z) = \frac{\mathbb{1}_S(z) \sqrt{\det \mathbf{G}^{-1}(z)}}{\int_{\mathbb{R}^d} \mathbb{1}_S(z) \sqrt{\det \mathbf{G}^{-1}(z)} dz},$$

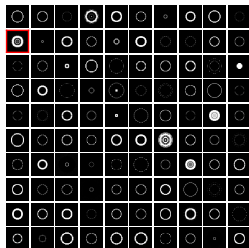
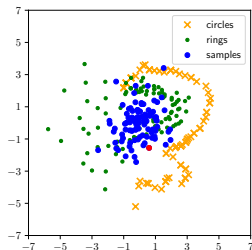
where  $S$  is a compact set and  $\mathbb{1}_S(z) = 1$  if  $z \in S$ , 0 otherwise.

- Use of classic MCMC sampler (e.g. Hamiltonian Monte Carlo)

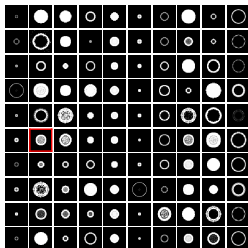
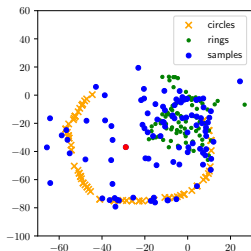
#### Pros:

- $\mathbf{G}^{-1}$  easily computable
- Samples “close” to the data

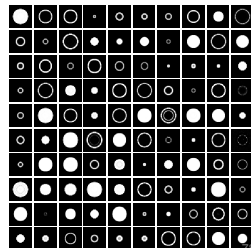
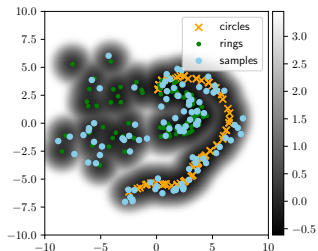
# Sampling Comparison

(a) VAE -  $\mathcal{N}(0, I)$ 

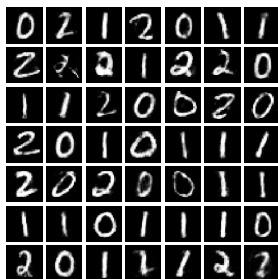
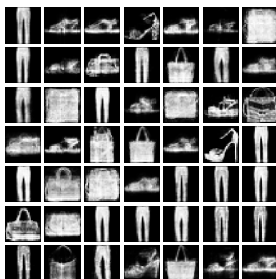
(b) VAE - VAMP (multimodal conditional prior)



(c) Ours



# Sampling Comparison - Higher Dimension

(a) *reduced* MNIST (120)(b) *reduced* EMNIST (120)(c) *reduced* Fashion (120)

# Data Augmentation

# Data Augmentation

1. Framework
2. Toy Data
3. Medical Imaging

# Data Augmentation - Framework

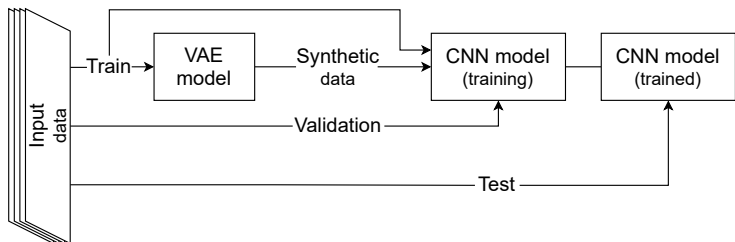


Figure: Data Augmentation pipeline

Performances are estimated using cross-validation.

# Data Augmentation

1. Framework
2. Toy Data
3. Medical Imaging

# Robustness Across Data Sets

Table: Classification results on *reduced* data sets ( $\sim 50$  samples per class)

	MNIST	MNIST (unbal.)	EMNIST (unbal.)	FASHION
Baseline	$89.9 \pm 0.6$	$81.5 \pm 0.7$	$82.6 \pm 1.4$	$76.0 \pm 1.5$
Baseline + Synthetic				
Basic Augmentation (X5)	$92.8 \pm 0.4$	$86.5 \pm 0.9$	$85.6 \pm 1.3$	$77.5 \pm 2.0$
Basic Augmentation (X10)	$88.2 \pm 2.2$	$82.0 \pm 2.4$	$85.7 \pm 0.3$	$79.2 \pm 0.6$
Basic Augmentation (X15)	$92.8 \pm 0.7$	$85.8 \pm 3.4$	$86.6 \pm 0.8$	$80.0 \pm 0.5$
VAE - 200*	$88.5 \pm 0.9$	$84.0 \pm 2.0$	$81.7 \pm 3.0$	$78.6 \pm 0.4$
VAE - 2k*	$92.2 \pm 1.6$	$88.0 \pm 2.2$	$86.0 \pm 0.2$	$79.3 \pm 1.1$
Ours-200	$91.0 \pm 1.0$	$84.1 \pm 2.0$	$85.1 \pm 1.1$	$77.0 \pm 0.8$
Ours-500	$92.3 \pm 1.1$	$87.7 \pm 0.9$	$85.1 \pm 1.1$	$78.5 \pm 0.9$
Ours-1k	$93.2 \pm 0.8$	<b><math>89.7 \pm 0.8</math></b>	$87.0 \pm 1.0$	<b><math>80.2 \pm 0.8</math></b>
Ours-2k	<b><math>94.3 \pm 0.8</math></b>	$89.1 \pm 1.9$	<b><math>87.6 \pm 0.8</math></b>	$78.1 \pm 1.8$

\* Using a standard normal prior to generate

# Robustness Across Data Sets

Table: Classification results on *reduced* data sets ( $\sim 50$  samples per class)

	MNIST	MNIST (unbal.)	EMNIST (unbal.)	FASHION
Baseline	$89.9 \pm 0.6$	$81.5 \pm 0.7$	$82.6 \pm 1.4$	$76.0 \pm 1.5$
Baseline + Synthetic				
Basic Augmentation (X5)	$92.8 \pm 0.4$	$86.5 \pm 0.9$	$85.6 \pm 1.3$	$77.5 \pm 2.0$
Basic Augmentation (X10)	$88.2 \pm 2.2$	$82.0 \pm 2.4$	$85.7 \pm 0.3$	$79.2 \pm 0.6$
Basic Augmentation (X15)	$92.8 \pm 0.7$	$85.8 \pm 3.4$	$86.6 \pm 0.8$	$80.0 \pm 0.5$
VAE - 200*	$88.5 \pm 0.9$	$84.0 \pm 2.0$	$81.7 \pm 3.0$	$78.6 \pm 0.4$
VAE - 2k*	$92.2 \pm 1.6$	$88.0 \pm 2.2$	$86.0 \pm 0.2$	$79.3 \pm 1.1$
Ours-200	$91.0 \pm 1.0$	$84.1 \pm 2.0$	$85.1 \pm 1.1$	$77.0 \pm 0.8$
Ours-500	$92.3 \pm 1.1$	$87.7 \pm 0.9$	$85.1 \pm 1.1$	$78.5 \pm 0.9$
Ours-1k	$93.2 \pm 0.8$	<b><math>89.7 \pm 0.8</math></b>	$87.0 \pm 1.0$	<b><math>80.2 \pm 0.8</math></b>
Ours-2k	<b><math>94.3 \pm 0.8</math></b>	$89.1 \pm 1.9$	<b><math>87.6 \pm 0.8</math></b>	$78.1 \pm 1.8$

\* Using a standard normal prior to generate

- Classic DA is data set dependent

# Robustness Across Data Sets

**Table:** Classification results on *reduced* data sets ( $\sim 50$  samples per class)

	MNIST	MNIST (unbal.)	EMNIST (unbal.)	FASHION
Baseline	$89.9 \pm 0.6$	$81.5 \pm 0.7$	$82.6 \pm 1.4$	$76.0 \pm 1.5$
Baseline + Synthetic				
Basic Augmentation (X5)	$92.8 \pm 0.4$	$86.5 \pm 0.9$	$85.6 \pm 1.3$	$77.5 \pm 2.0$
Basic Augmentation (X10)	$88.2 \pm 2.2$	$82.0 \pm 2.4$	$85.7 \pm 0.3$	$79.2 \pm 0.6$
Basic Augmentation (X15)	$92.8 \pm 0.7$	$85.8 \pm 3.4$	$86.6 \pm 0.8$	$80.0 \pm 0.5$
VAE - 200*	$88.5 \pm 0.9$	$84.0 \pm 2.0$	$81.7 \pm 3.0$	$78.6 \pm 0.4$
VAE - 2k*	$92.2 \pm 1.6$	$88.0 \pm 2.2$	$86.0 \pm 0.2$	$79.3 \pm 1.1$
Ours-200	$91.0 \pm 1.0$	$84.1 \pm 2.0$	$85.1 \pm 1.1$	$77.0 \pm 0.8$
Ours-500	$92.3 \pm 1.1$	$87.7 \pm 0.9$	$85.1 \pm 1.1$	$78.5 \pm 0.9$
Ours-1k	$93.2 \pm 0.8$	<b><math>89.7 \pm 0.8</math></b>	$87.0 \pm 1.0$	<b><math>80.2 \pm 0.8</math></b>
Ours-2k	<b><math>94.3 \pm 0.8</math></b>	$89.1 \pm 1.9$	<b><math>87.6 \pm 0.8</math></b>	$78.1 \pm 1.8$

\* Using a standard normal prior to generate

- Classic DA is data set dependent
- Vanilla VAE performs as well as classic DA

# Robustness Across Data Sets

Table: Classification results on *reduced* data sets ( $\sim 50$  samples per class) **on synthetic samples only**

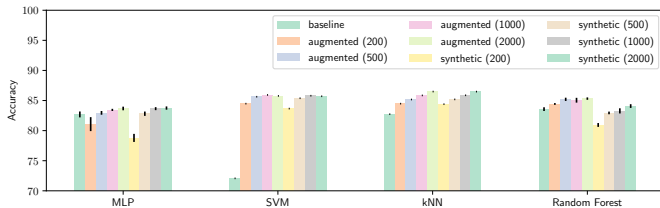
	MNIST	MNIST (unbal.)	EMNIST (unbal.)	FASHION
Baseline	$89.9 \pm 0.6$	$81.5 \pm 0.7$	$82.6 \pm 1.4$	$76.0 \pm 1.5$
Synthetic Only				
VAE - 200*	$69.9 \pm 1.5$	$64.6 \pm 1.8$	$65.7 \pm 2.6$	$73.9 \pm 3.0$
VAE - 2k*	$86.5 \pm 2.2$	$79.6 \pm 3.8$	$78.8 \pm 3.0$	$76.7 \pm 1.6$
Ours-200	$87.2 \pm 1.1$	$79.5 \pm 1.6$	$77.0 \pm 1.6$	$77.0 \pm 0.8$
Ours-500	$89.1 \pm 1.3$	$80.4 \pm 2.1$	$80.2 \pm 2.0$	$78.5 \pm 0.8$
Ours-1k	$90.1 \pm 1.4$	$86.2 \pm 1.8$	$82.6 \pm 1.3$	$79.3 \pm 0.6$
Ours-2k	$92.6 \pm 1.1$	$87.5 \pm 1.3$	$86.0 \pm 1.0$	$78.3 \pm 0.9$

\* Using a standard normal prior to generate

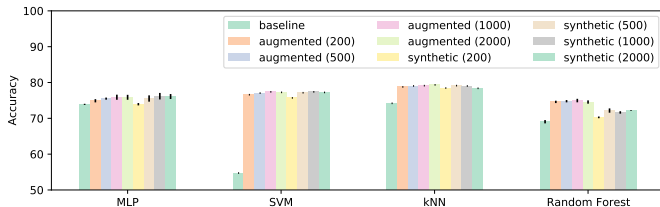
- The proposed model seems to create diverse samples relevant to the classifier

# Robustness Across Classifiers

(a) *reduced* MNIST balanced



(b) *reduced* MNIST unbalanced



# A Note on the Method Scalability

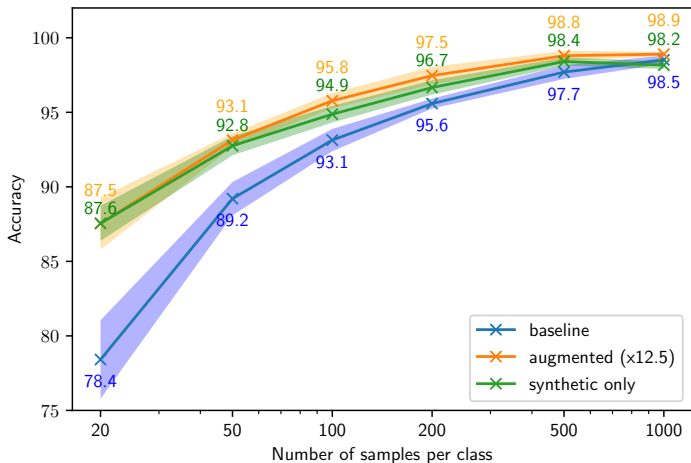


Figure: Benchmark classifier accuracy according to the number of samples in the training set on MNIST.

# Data Augmentation

1. Framework
2. Toy Data
3. Medical Imaging

## Datasets and classification task

Classification task: Alzheimer's disease patients (**AD**) vs Cognitively Normal participants (**CN**) using T1-weighted MR images.



**Table:** Summary of participant demographics, mini-mental state examination (MMSE) and global clinical dementia rating (CDR) scores at baseline.

Data set	Label	Obs.	Age	Sex M/F	MMSE	CDR
ADNI	CN	403	73.3 ± 6.0	185/218	29.1 ± 1.1	0: 403
	AD	362	74.9 ± 7.9	202/160	23.1 ± 2.1	0.5: 169, 1: 192, 2: 1
AIBL	CN	429	73.0 ± 6.2	183/246	28.8 ± 1.2	0: 406, 0.5: 22, 1: 1
	AD	76	74.4 ± 8.0	33/43	20.6 ± 5.5	0.5: 31, 1: 36, 2: 7, 3: 2

# MRI preprocessing

Bias field correction (N4ITK) + linear registration (ANTs) + cropping

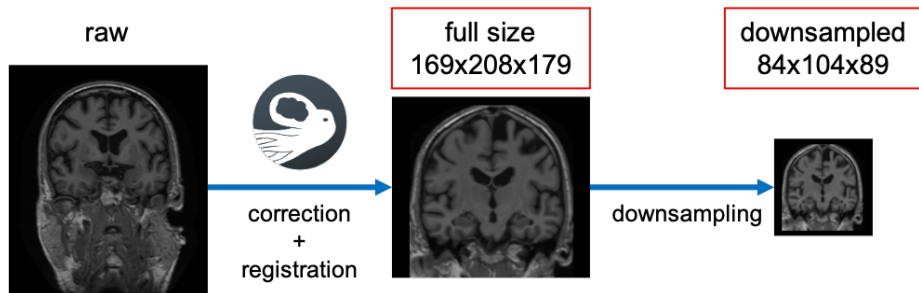
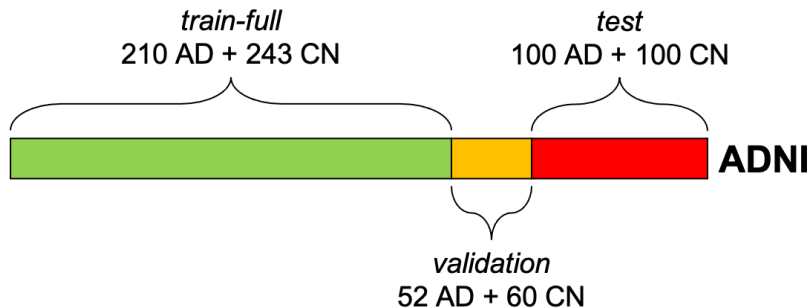


Figure: Preprocessed MRI used in the study

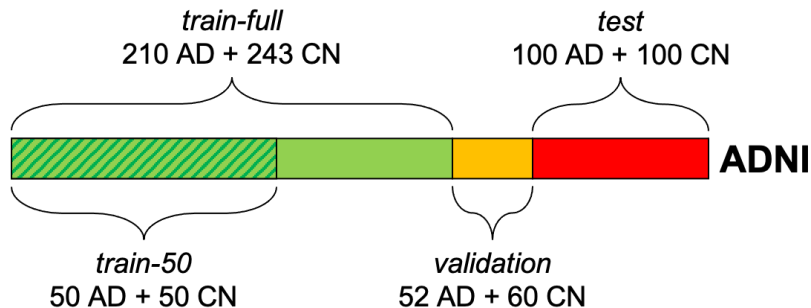
Find wonderful data at:

`/network/lustre/dtlake01/aramis/datasets/adni/caps/caps_v2021`

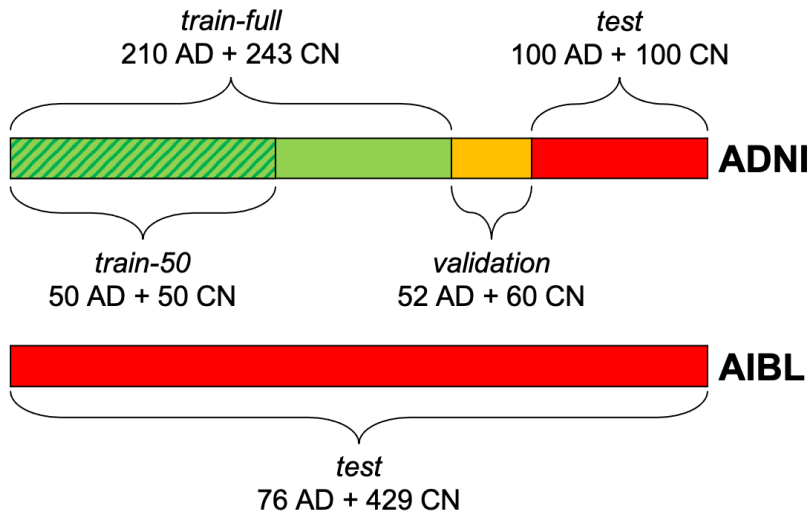
# Evaluation procedure



# Evaluation procedure



# Evaluation procedure



# CNN architectures

Baseline architectures provided by a previous study [WTSDM<sup>+</sup>20]

## 1. Full size image



## 2. Downsampled image



3D Convolution (stride=1, padding=1) + Batch normalization + LeakyReLU

MaxPooling (kernel=2, stride=2)

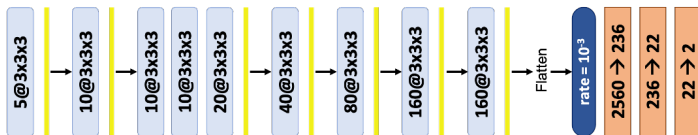
Dropout

Fully-connected layer (+ LeakyReLU except last layer)

# CNN architectures

**Optimized** architectures optimize with **random search procedure** for this training set (ClinicaDL)

## 1. Full size image



## 2. Downsampled image



3D Convolution (stride=1, padding=1) + Batch normalization + LeakyReLU

MaxPooling (kernel=2, stride=2)

Dropout

Fully-connected layer (+ LeakyReLU except last layer)

# Experiments

Four series of experiments:

- **baseline** architecture on *train-50*
- **baseline** architecture on *train-full*
- **optimized** architecture on *train-50*
- **optimized** architecture on *train-full*

For each experiment 20 CNNs are run and the performance is the mean value of the 20 performance values.

# Synthesized images

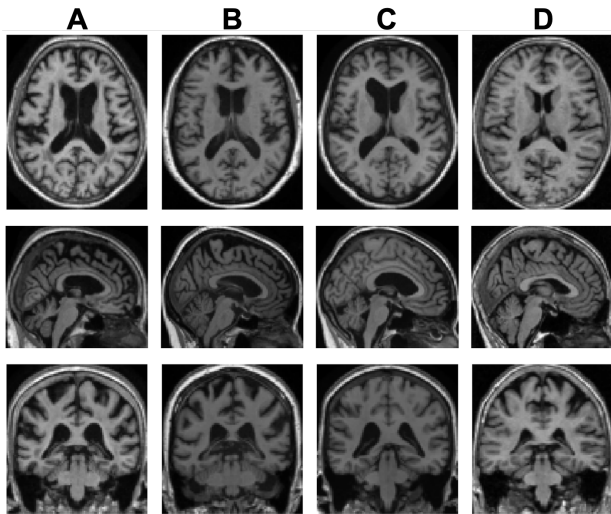


**Figure:** Example of two *true* patients compared to two generated by our method. Can you find the intruders ?

# Synthesized images

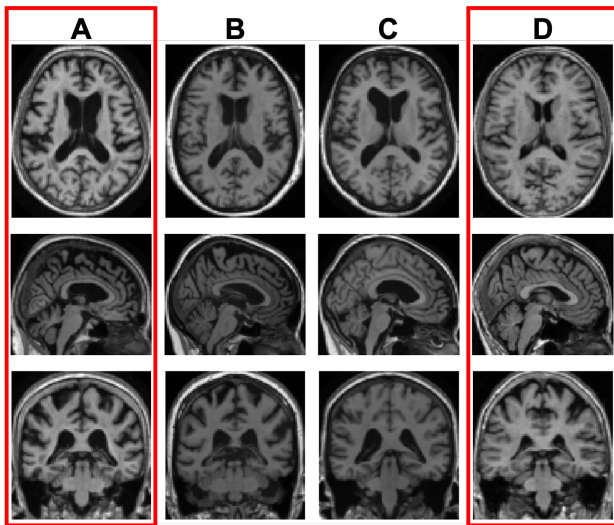


**Figure:** Example of two *true* patients compared to two generated by our method. Can you find the intruders ?

## Results on train-50 with baseline CNN

**Table:** Mean test performance of each series of 20 runs trained with the **baseline** hyperparameters on *train-50* set.

data set	ADNI balanced accuracy	AIBL balanced accuracy
real	$66.3 \pm 2.4$	$67.2 \pm 4.1$
real (high-resolution)	$67.9 \pm 2.3$	$66.5 \pm 3.0$
500 synthetic + real	$69.4 \pm 1.6$	$68.5 \pm 2.5$
1000 synthetic + real	$70.5 \pm 2.1$	$70.6 \pm 3.1$
2000 synthetic + real	$71.2 \pm 1.6$	$72.8 \pm 2.2$
3000 synthetic + real	$72.6 \pm 1.6$	$73.6 \pm 3.0$
5000 synthetic + real	<b><math>74.1 \pm 2.2</math></b>	<b><math>76.1 \pm 3.6</math></b>
10000 synthetic + real	$74.0 \pm 2.7$	$74.9 \pm 3.2$

Increase of balanced accuracy of 6.2 points on ADNI and 8.9 points on AIBL

## Results on train-full with baseline CNN

**Table:** Mean test performance of each series of 20 runs trained with the **baseline** hyperparameters on *train-full* set.

data set	ADNI balanced accuracy	AIBL balanced accuracy
real	$77.7 \pm 2.5$	$78.4 \pm 2.4$
real (high-resolution)	$80.6 \pm 1.1$	$80.4 \pm 2.6$
500 synthetic + real	$82.2 \pm 2.4$	$82.9 \pm 2.5$
1000 synthetic + real	$84.4 \pm 1.8$	$83.7 \pm 2.3$
2000 synthetic + real	$85.9 \pm 1.6$	$83.8 \pm 2.2$
3000 synthetic + real	$85.8 \pm 1.7$	$84.4 \pm 1.8$
5000 synthetic + real	$85.7 \pm 2.1$	$84.2 \pm 2.2$
10000 synthetic + real	<b><math>86.3 \pm 1.8</math></b>	<b><math>85.1 \pm 1.9</math></b>

Increase of balanced accuracy of 5.7 points on ADNI and 4.7 on AIBL

## Results on train-50 with optimized CNN

**Table:** Mean test performance of each series of 20 runs trained with the **baseline** hyperparameters on *train-50* set.

data set	ADNI balanced accuracy	AIBL balanced accuracy
real	$75.5 \pm 2.7$	$75.6 \pm 4.1$
real (high-resolution)	$72.1 \pm 3.1$	$71.2 \pm 5.1$
500 synthetic + real	$75.6 \pm 2.5$	$76.0 \pm 4.2$
1000 synthetic + real	$77.8 \pm 2.3$	$80.9 \pm 3.2$
2000 synthetic + real	$76.9 \pm 2.4$	$80.0 \pm 3.6$
3000 synthetic + real	$77.8 \pm 1.9$	$81.2 \pm 3.7$
5000 synthetic + real	$76.9 \pm 2.5$	$80.9 \pm 2.7$
10000 synthetic + real	<b><math>78.0 \pm 2.1</math></b>	<b><math>81.9 \pm 2.2</math></b>

Increase of balanced accuracy of 2.5 points on ADNI and 6.3 points on AIBL

## Results on train-full with optimized CNN

**Table:** Mean test performance of each series of 20 runs trained with the **baseline** hyperparameters on *train-full* set.

data set	ADNI balanced accuracy	AIBL balanced accuracy
real	$85.5 \pm 2.4$	$81.9 \pm 3.2$
real (high-resolution)	$85.7 \pm 2.5$	$84.4 \pm 1.7$
500 synthetic + real	$86.0 \pm 1.8$	$83.2 \pm 2.4$
1000 synthetic + real	$86.5 \pm 1.9$	$83.7 \pm 2.0$
2000 synthetic + real	<b><math>87.2 \pm 1.7</math></b>	$84.0 \pm 2.0$
3000 synthetic + real	$85.8 \pm 2.6$	$83.6 \pm 3.2$
5000 synthetic + real	$86.4 \pm 1.3$	$83.5 \pm 2.2$
10000 synthetic + real	$86.7 \pm 1.8$	<b><math>84.3 \pm 1.8</math></b>

Increase of balanced accuracy of 1.5 point on ADNI and -0.1 point on AIBL

# Conclusion

We have proposed

- a new geometry aware VAE-based data augmentation framework relevant for representing and classifying data in the HDLSS setting.
- Validated on classification tasks on *toy* and *real-life* data sets.

# Conclusion

We have proposed

- a **new geometry aware VAE-based data augmentation framework** relevant for representing and classifying data in the HDLSS setting.
- Validated on classification tasks on *toy* and *real-life* data sets.

Strengths:

- **Independent on the nature of the data set:** from 2D images (MNIST, EMNIST, FASHION) to 3D medical images (ADNI and AIBL),
- **Relevant synthetic data:** classifiers achieved a similar or better classification performance when trained only on synthetic data than on the *real* train set.
- **Classifier independence:** MLP, random forest, k-NN and SVM (on toy data sets) ; baseline and optimized parameters (on medical images).

# Conclusion

We have proposed

- a **new geometry aware VAE-based data augmentation framework** relevant for representing and classifying data in the HDLSS setting.
- Validated on classification tasks on *toy* and *real-life* data sets.

Limitations - what could be improved:

- No extensive search on VAE architecture.
- Would it benefit from the use of longitudinal data?
- *train-50* is still large compared to some medical data sets. . .

# Implementation

All this is available as a Python library named [Pyraug](#):

Training Pipeline:

```
>>> from pyraug.pipelines import TrainingPipeline
>>> pipeline = TrainingPipeline()
>>> pipeline(train_data=dataset_to_augment)
```

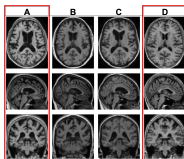
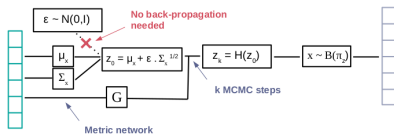
Data sampler:

```
>>> from pyraug.pipelines import GenerationPipeline
>>> from pyraug.models import RHVAE
>>> model = RHVAE.load_from_folder('path/to/your/trained/model') # reload the model
>>> pipe = GenerationPipeline(model=model) # define pipeline
>>> pipe(samples_number=10) # This will generate 10 data points
```

The logo for PyRaug, featuring the word 'PyRaug' in a stylized, handwritten font. The 'Py' is in a smaller, lighter font, and 'Raug' is in a larger, bolder font. The letters are slightly overlapping and have a soft, glowing effect.

Available (upon request by email) and soon for download under licence on Pypi and github with documentation and tutorials.

# Thank you!



Contacts:

clement.chadebec@inria.fr  
 stephanie.allasonniere@u-paris.fr

# References I

-  Christoph Baur, Shadi Albarqouni, and Nassir Navab, *Generating highly realistic images of skin lesions with GANs*, OR 2.0 Context-Aware Operating Theaters, Computer Assisted Robotic Endoscopy, Clinical Image-Based Procedures, and Skin Image Analysis, Springer, 2018, pp. 260–267.
-  Lei Bi, Jinman Kim, Ashnil Kumar, Dagan Feng, and Michael Fulham, *Synthesis of Positron Emission Tomography (PET) Images via Multi-channel Generative Adversarial Networks (GANs)*, Molecular Imaging, Reconstruction and Analysis of Moving Body Organs, and Stroke Imaging and Treatment, LNCS, Springer, 2017, pp. 43–51.
-  Anthony L Caterini, Arnaud Doucet, and Dino Sejdinovic, *Hamiltonian variational auto-encoder*, Advances in Neural Information Processing Systems, 2018, pp. 8167–8177.
-  Clment Chadebec, Clment Mantoux, and Stphanie Allasonnire, *Geometry-aware hamiltonian variational auto-encoder*, arXiv:2010.11518 [cs, math, stat] (2020).

## References II

-  Francesco Calimeri, Aldo Marzullo, Claudio Stamile, and Giorgio Terracina, *Biomedical data augmentation using generative adversarial neural networks*, International conference on artificial neural networks, Springer, 2017, pp. 626–634.
-  Clément Chadebec, Elina Thibeau-Sutre, Ninon Burgos, and Stéphanie Allasonnière, *Data augmentation in high dimensional low sample size setting using a geometry-based variational autoencoder*, arXiv preprint arXiv:2105.00026 (2021).
-  Alain Durmus, Eric Moulines, and Eero Saksman, *On the convergence of hamiltonian monte carlo*, arXiv preprint arXiv:1705.00166 (2017).
-  Maayan Frid-Adar, Idit Diamant, Eyal Klang, Michal Amitai, Jacob Goldberger, and Hayit Greenspan, *GAN-based synthetic medical image augmentation for increased CNN performance in liver lesion classification*, Neurocomputing **321** (2018), 321–331.

## References III

-  Mark Girolami and Ben Calderhead, *Riemann manifold langevin and hamiltonian monte carlo methods*, Journal of the Royal Statistical Society: Series B (Statistical Methodology) **73** (2011), no. 2, 123–214.
-  Mark Girolami, Ben Calderhead, and Siu A Chin, *Riemannian manifold hamiltonian monte carlo*, arXiv preprint arXiv:0907.1100 (2009).
-  Dimitrios Korkinof, Tobias Rijken, Michael O'Neill, Joseph Yearsley, Hugh Harvey, and Ben Glocker, *High-resolution mammogram synthesis using progressive generative adversarial networks*, arXiv preprint arXiv:1807.03401 (2018).
-  Diederik P. Kingma and Max Welling, *Auto-encoding variational bayes*, arXiv:1312.6114 [cs, stat] (2014).
-  Samuel Livingstone, Michael Betancourt, Simon Byrne, Mark Girolami, and others, *On the geometric ergodicity of hamiltonian monte carlo*, Bernoulli **25** (2019), no. 4, 3109–3138.

## References IV

-  Maxime Louis, *Computational and statistical methods for trajectory analysis in a Riemannian geometry setting*, PhD Thesis, Sorbonnes universits, 2019.
-  Yufei Liu, Yuan Zhou, Xin Liu, Fang Dong, Chang Wang, and Zihong Wang, *Wasserstein gan-based small-sample augmentation for new-generation artificial intelligence: a case study of cancer-staging data in biology*, *Engineering* **5** (2019), no. 1, 156–163.
-  Ali Madani, Mehdi Moradi, Alexandros Karargyris, and Tanveer Syeda-Mahmood, *Chest x-ray generation and data augmentation for cardiovascular abnormality classification*, *Medical Imaging 2018: Image Processing*, vol. 10574, International Society for Optics and Photonics, 2018, p. 105741M.
-  Radford M Neal and others, *MCMC using hamiltonian dynamics*, *Handbook of Markov Chain Monte Carlo* **2** (2011), no. 11, 2.

# References V

-  Danilo Rezende and Shakir Mohamed, *Variational inference with normalizing flows*, International Conference on Machine Learning, PMLR, 2015, pp. 1530–1538.
-  Danilo Jimenez Rezende, Shakir Mohamed, and Daan Wierstra, *Stochastic backpropagation and approximate inference in deep generative models*, International conference on machine learning, PMLR, 2014, pp. 1278–1286.
-  Hoo-Chang Shin, Neil A Tenenholtz, Jameson K Rogers, Christopher G Schwarz, Matthew L Senjem, Jeffrey L Gunter, Katherine P Andriole, and Mark Michalski, *Medical image synthesis for data augmentation and anonymization using generative adversarial networks*, International Workshop on Simulation and Synthesis in Medical Imaging, LNCS, Springer, 2018, pp. 1–11.

## References VI

-  Hojjat Salehinejad, Shahrokh Valaee, Tim Dowdell, Errol Colak, and Joseph Barfett, *Generalization of deep neural networks for chest pathology classification in x-rays using generative adversarial networks*, 2018 IEEE International Conference on Acoustics, Speech and Signal Processing (ICASSP), IEEE, 2018, pp. 990–994.
-  Veit Sandfort, Ke Yan, Perry J. Pickhardt, and Ronald M. Summers, *Data augmentation using generative adversarial networks (CycleGAN) to improve generalizability in CT segmentation tasks*, Scientific reports **9** (2019), no. 1, 16884.
-  Abdul Waheed, Muskan Goyal, Deepak Gupta, Ashish Khanna, Fadi Al-Turjman, and Plcido Rogerio Pinheiro, *Covidgan: data augmentation using auxiliary classifier gan for improved covid-19 detection*, IEEE Access **8** (2020), 91916–91923.

## References VII

-  Junhao Wen, Elina Thibeau-Sutre, Mauricio Diaz-Melo, Jorge Samper-Gonzlez, Alexandre Routier, Simona Bottani, Didier Dormont, Stanley Durrleman, Ninon Burgos, and Olivier Colliot, *Convolutional neural networks for classification of Alzheimer's disease: Overview and reproducible evaluation*, *Medical Image Analysis* **63** (2020), 101694.
-  Eric Wu, Kevin Wu, David Cox, and William Lotter, *Conditional infilling gans for data augmentation in mammogram classification*, *Image analysis for moving organ, breast, and thoracic images*, Springer, 2018, pp. 98–106.
-  Xin Yi, Ekta Walia, and Paul Babyn, *Generative adversarial network in medical imaging: A review*, *Medical image analysis* **58** (2019), 101552.





# Clustering

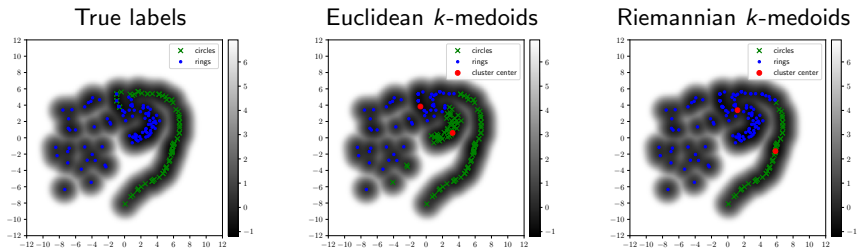


Figure: Euclidean and Riemannian  $k$ -medoids clustering.

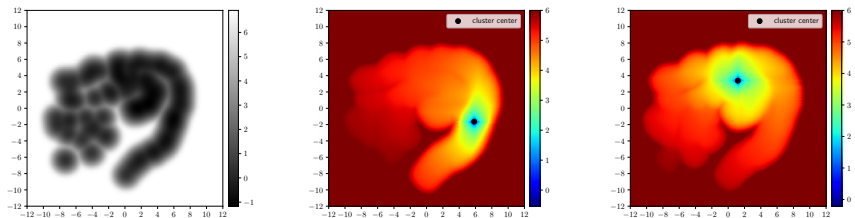


Figure: Distance maps.

# Results - Clustering

Data set	Model	Subset 1	Subset 2	Subset 3	Mean
Synthetic data	linear	53.88	62.52	71.63	62.68
	geodesic	<b>71.41</b>	<b>81.39</b>	<b>79.49</b>	<b>77.43</b>
MNIST 1	linear	89.73	93.11	91.80	91.55
	geodesic	<b>91.68</b>	<b>94.51</b>	<b>95.63</b>	<b>93.94</b>
MNIST 2	linear	68.24	69.22	79.05	71.17
	geodesic	<b>70.35</b>	<b>71.34</b>	<b>79.64</b>	<b>73.78</b>
MNIST 3	linear	75.55	75.76	81.70	77.67
	geodesic	<b>76.08</b>	<b>77.94</b>	<b>81.96</b>	<b>78.66</b>
FashionMNIST 1	linear	90.47	91.63	86.78	89.63
	geodesic	<b>91.44</b>	<b>92.55</b>	<b>87.46</b>	<b>90.48</b>
FashionMNIST 2	linear	92.20	91.26	93.30	92.25
	geodesic	<b>93.56</b>	<b>91.80</b>	<b>94.12</b>	<b>93.16</b>
FashionMNIST 3	linear	72.46	79.58	83.16	78.40
	geodesic	<b>74.89</b>	<b>81.88</b>	<b>84.83</b>	<b>80.53</b>

Table: F1-Scores.